UNIVERSITÄT LEIPZIG

Remote sensing of clouds and snow properties in the Arctic

A.Ehrlich, T. Carlsen, E. Bierwirth, M. Wendisch
Leipzig Institute for Meteorology (LIM), University Leipzig, Germany
a.ehrlich@uni-leipzig.de

Fig. 1: MODIS satellite image of clouds, snow and sea ice in the Beaufort Sea (2012/05/05) illustrated in RGB colors (left) and false colors using chanel 7-2-1 (right).

1. Introduction

Retrieval of cloud and snow properties

- Spectral solar radiation contains information on clouds and snow

Snow Albedo	➡	Snow Grain Size, (soot)
Cloud Albedo	➡	Opt. Thickness, Effective Radius, (Phase)

- Spectral absorption of snow ice and cloud water not independent
- Assumptions on either clouds or snow properties needed

  A) Limitation of grain size retrieval due to cloud mask
  B) Limitation of cloud retrieval due to surface albedo

- Frequent low level clouds over Arctic sea ice or Antarctic ice shield
- Large areas are currently not well covered

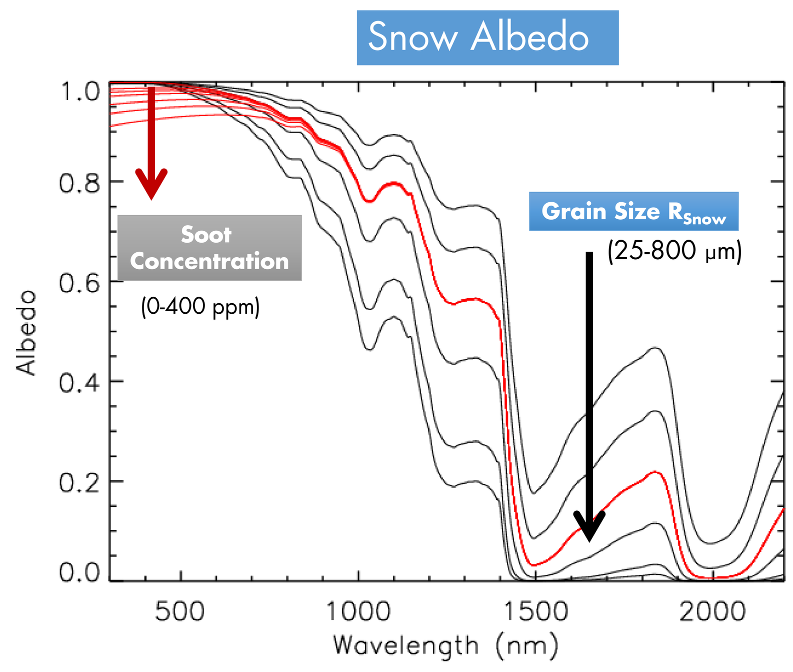

Fig. 2: Simulated spectral snow albedo in dependence of grain size and soot concentration.

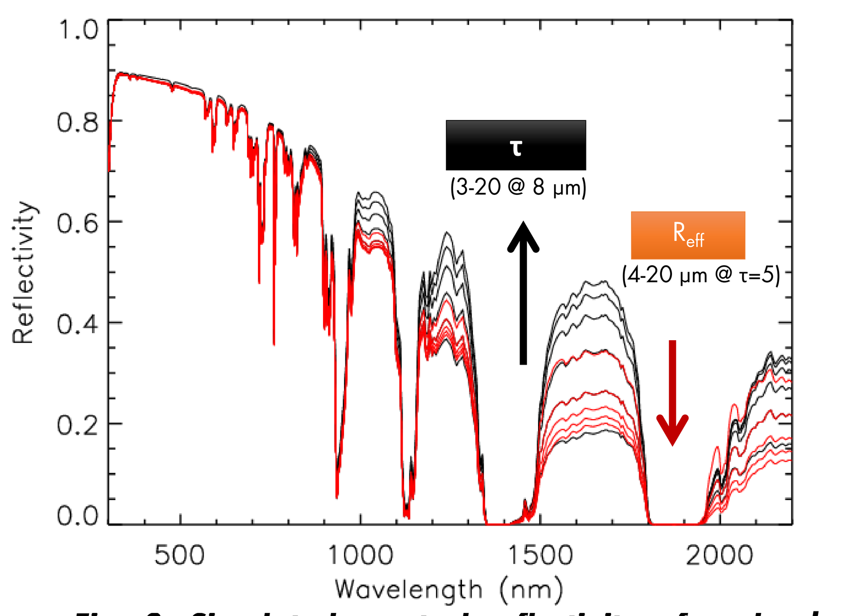

Fig. 3: Simulated spectral reflectivity of a cloud over snow in dependence of cloud optical thickness and cloud particle size.

2. Limitation of Cloud Retrieval

- Low contrast between snow and clouds (visible wavelength)
  ➔ Bi-spectral retrieval using near infrared wavelength (e.g., MODIS 1.6 µm/2.1 µm)
- Uncertainty due to assumed snow grain size
- Sensitivity study based on simulations:
  - Grain size assumed in retrieval: 200 µm / 50 µm
  - Grain size in reality: 50 µm / 200 µm

  \+ (Symbol in Fig 5) *
- Results:
  - Differences especially for thin clouds
  - Up to 40 % for opt. thickness
  - Up to 50 % for effective radius

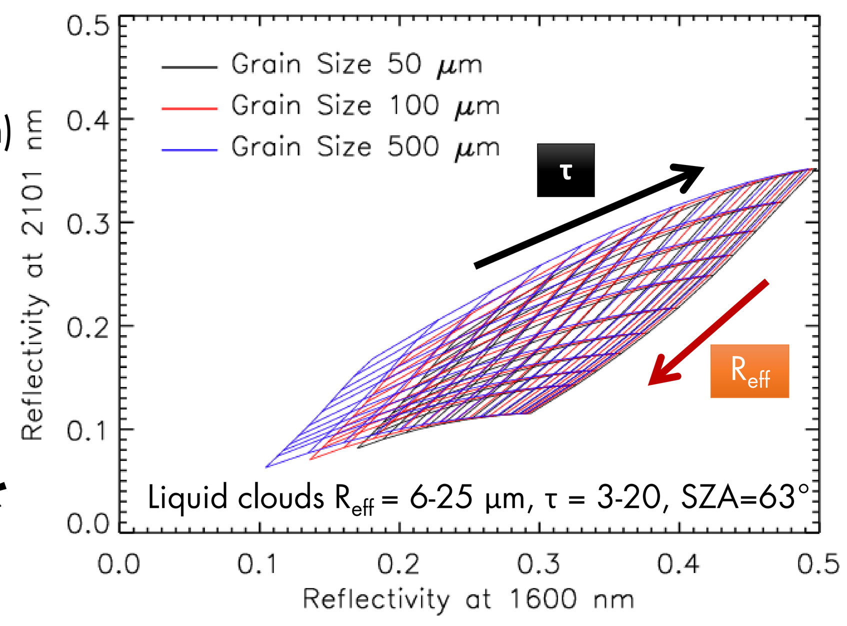

Fig. 4: Bi-spectral retrieval grid of cloud nadir reflectivity for clouds above snow assuming three different grain sizes.

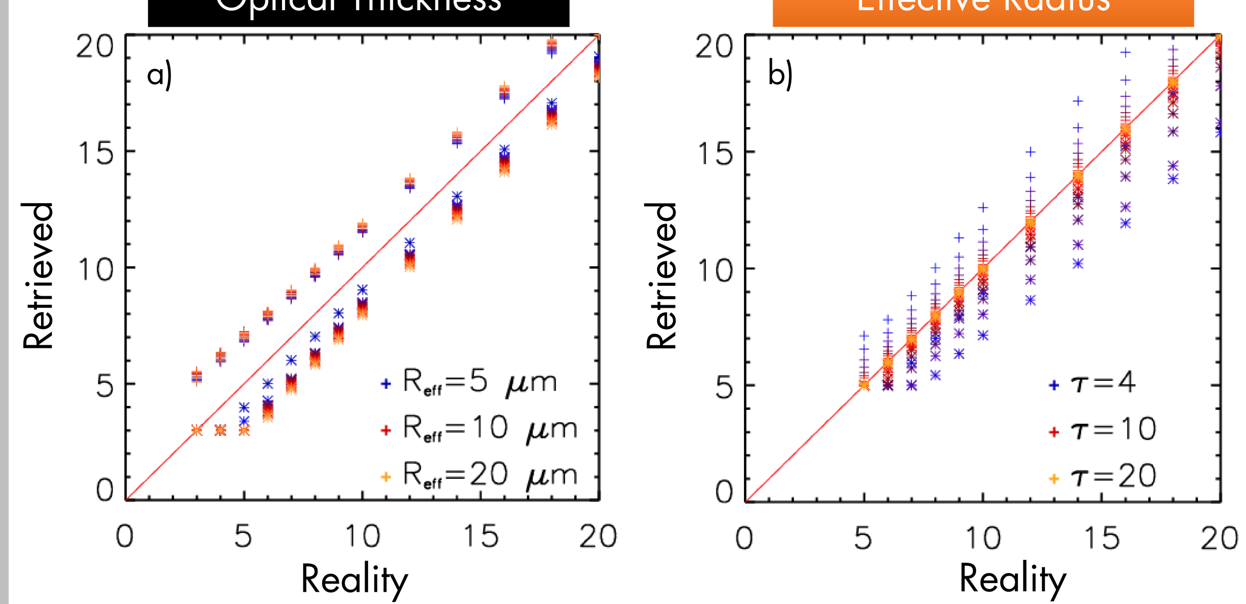

Fig. 5: Comparison of retrieved (synthetic data) and real cloud optical thickness (a) and droplet effective radius (b) when snow grain size is overestimated with 200 µm compared to reality with 50 µm (plus symbols) or underestimated with 50 µm compared to reality with 200 µm (asterisks).

3. Separating the Spectral Signature of Clouds and Snow

Simulations of nadir reflectivity

- Cloud altitude 300 - 500 m, θ_0 = 63°
- τ = 1 – 20
- R_{eff} = 2 – 25 µm
- R_{snow} = 10 – 800 µm (Zege et al., 2011)

- Impact of τ, R_{eff}, R_{snow} spectrally differs
- Visible wavelengths almost invariant
- Absorption by snow stronger than by cloud particles
  → R_{snow} affects shorter wavelengths
- τ increases reflectivity only above λ>1 µm

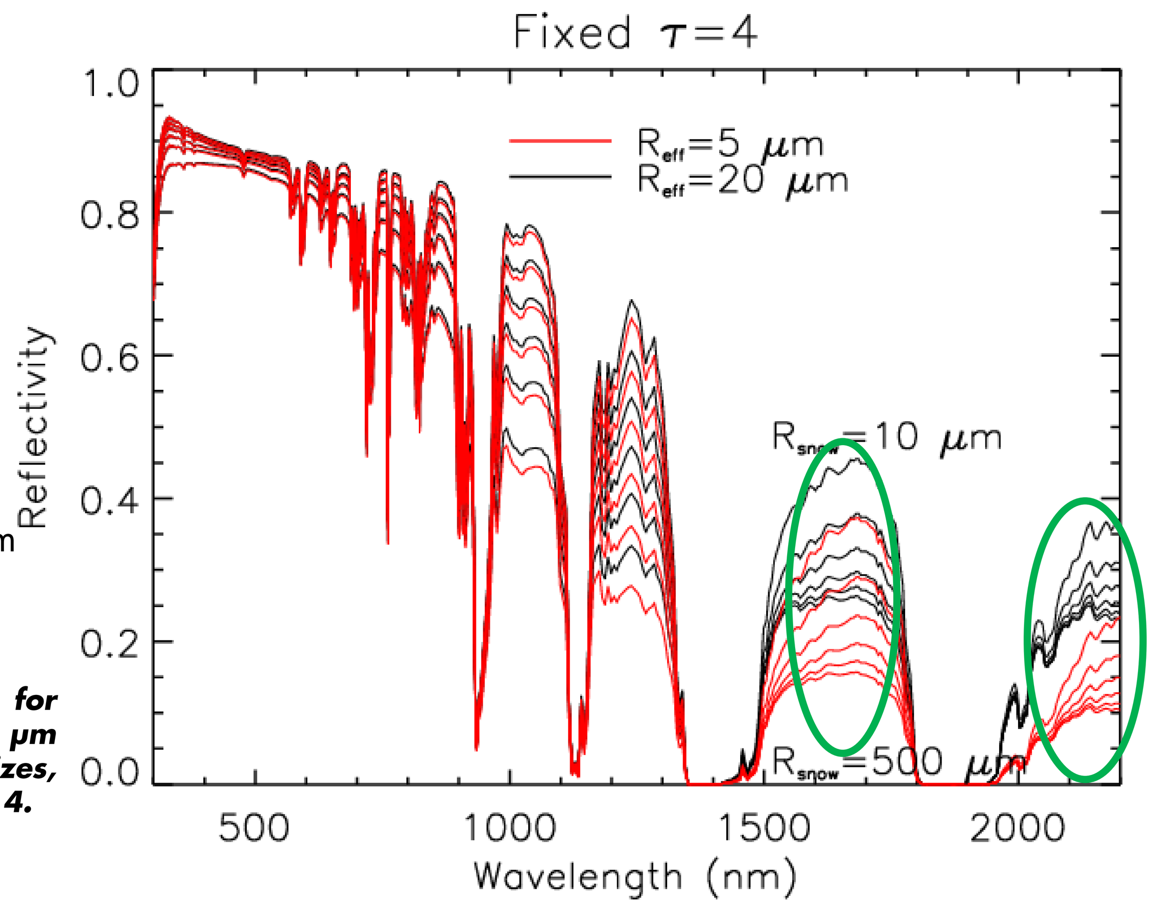

Fig. 6: Spectral nadir cloud reflectivity for different cloud droplet effective radii, 5 µm (red) and 20 µm (black) and snow grain sizes, 10-500 µm. The optical thickness is fixed to 4.

Spectral sensitivity with respect to cloud and snow properties

- Standard deviation and principle component analysis (PCA)
- Different spectral signature for τ, R_{eff}, and R_{snow}
- Maximum variability is clearly separated

R_{Snow}	980 – 1080 nm
τ	1550 – 1780 nm
R_{eff}	2000 – 2200 nm

- R_{snow} dominates at λ > 1 µm
- 3 main principle components found
  → linked to τ, R_{eff}, and R_{snow}

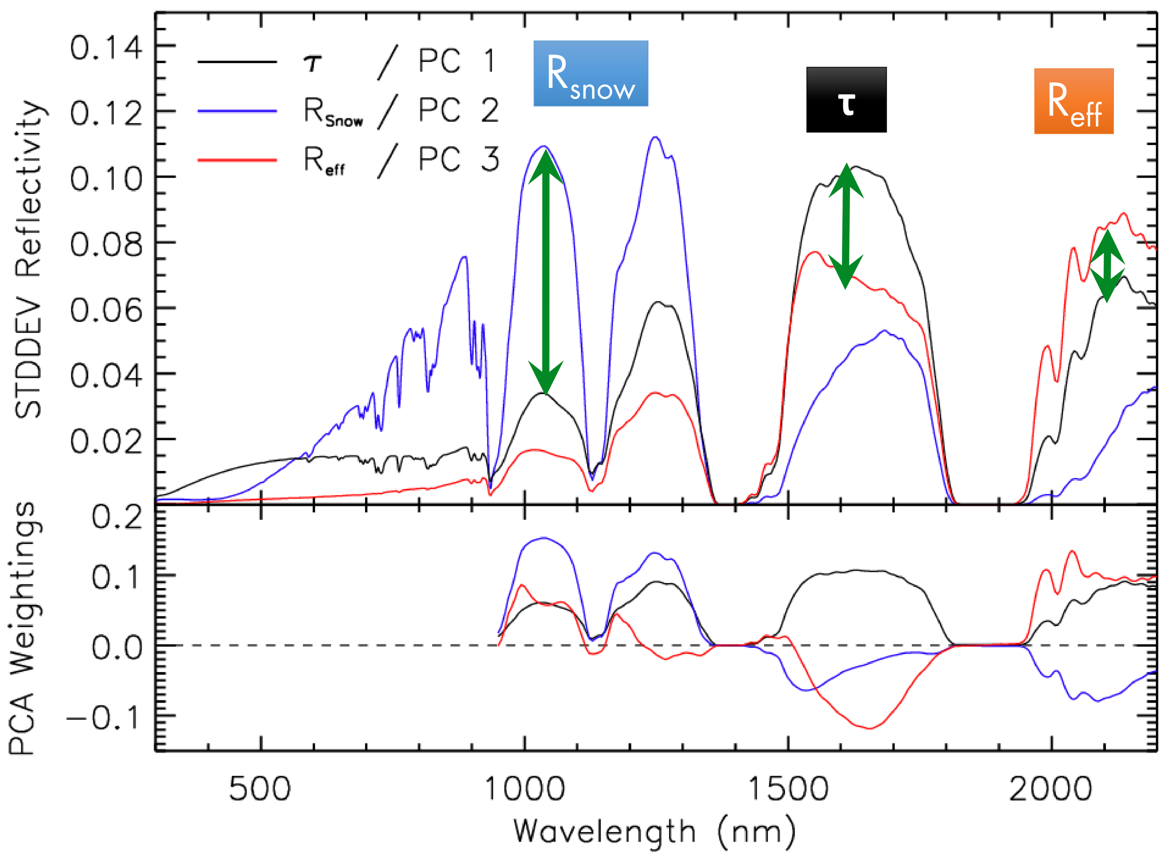

Fig. 7: Mean standard deviation of nadir cloud reflectivity with respect to a single input parameter τ, R_{eff}, and R_{snow} calculated for the sets of radiative transfer simulations. Weightings of a principle component analysis are given in the lower panel.

4. Reflectivity-Ratio Retrieval Algorithm

Reflectivity ratios

P1 = R(1040nm)/R(500nm)	➡	R_{Snow}
P2 = R(1655nm)/R(1040nm)	➡	τ
P3 = R(2100nm)/R(1655nm)	➡	R_{eff}

- Based on Werner et al. 2013, Brückner et al. 2014
- Reduces the impact of measurement uncertainties

Retrieval grid

- Forward simulations (θ_0 = 63°, cloud altitude 300 - 500 m)
- Almost orthogonal grids
- Separation of parameters
- Ambiguity only for R_{eff} < 4 µm (removed in Fig. 8)

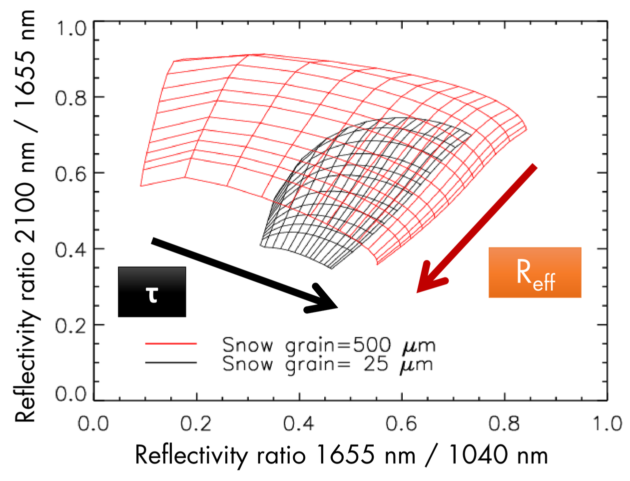

Fig. 8: Retrieval grids built by the three reflectivity ratios P1-3 calculated from forward simulations (solar zenith angle 63°, cloud base 300 m, cloud top 500 m).

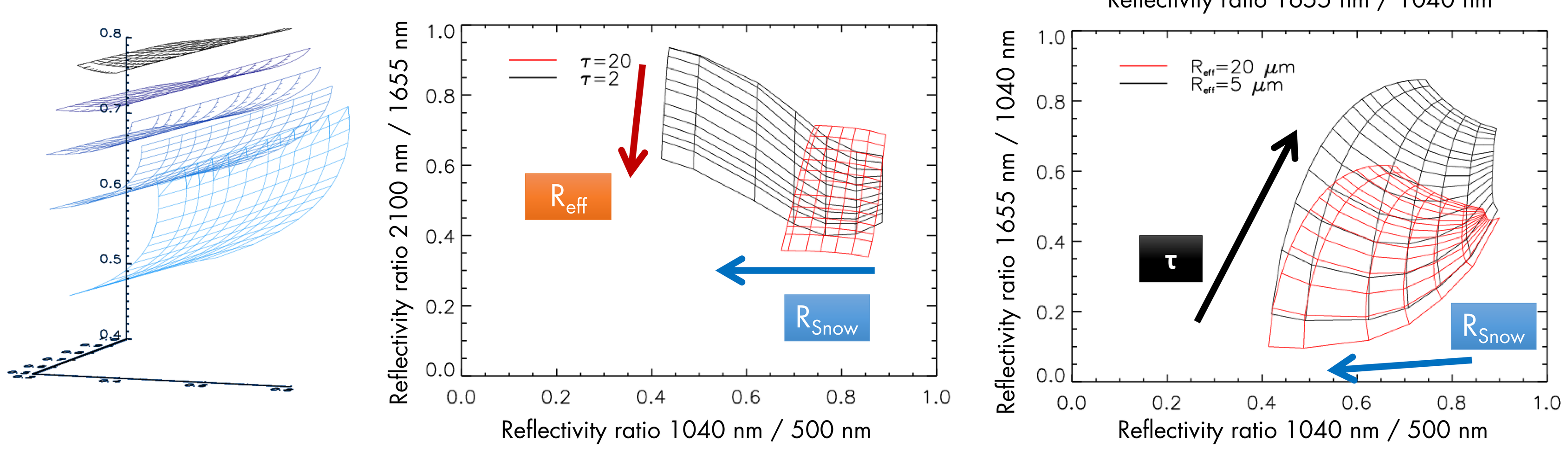

5. Application

VERDI 2012 campaign

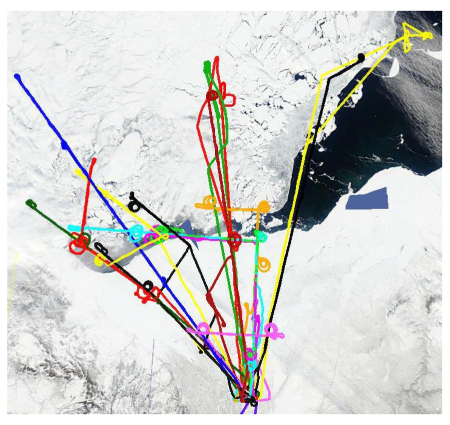

- Inuvik/NWT/Canada, April/May 2012
- Polar 5 aircraft of AWI
- Remote sensing
- In-situ cloud, aerosol and trace gases
- SMART-Albedometer
  - Spectral radiance
  - 300 - 2100 nm
  - 2-15 nm resolution
  - Horizontally stabilized

Case study 17 May 2012

- Homogeneous stratus (liquid)
- Flight track crossing ice edge
- Continuous retrieval results
- Large grain size likely due to sea ice and melting

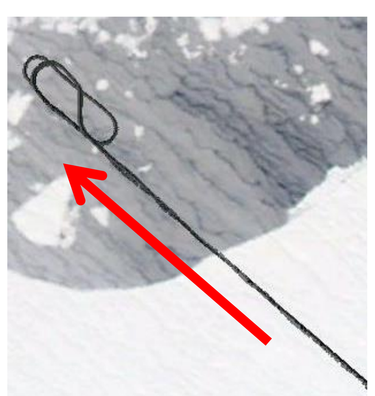

Fig. 9: Flight track analysed in the case study of 17 May 2012.

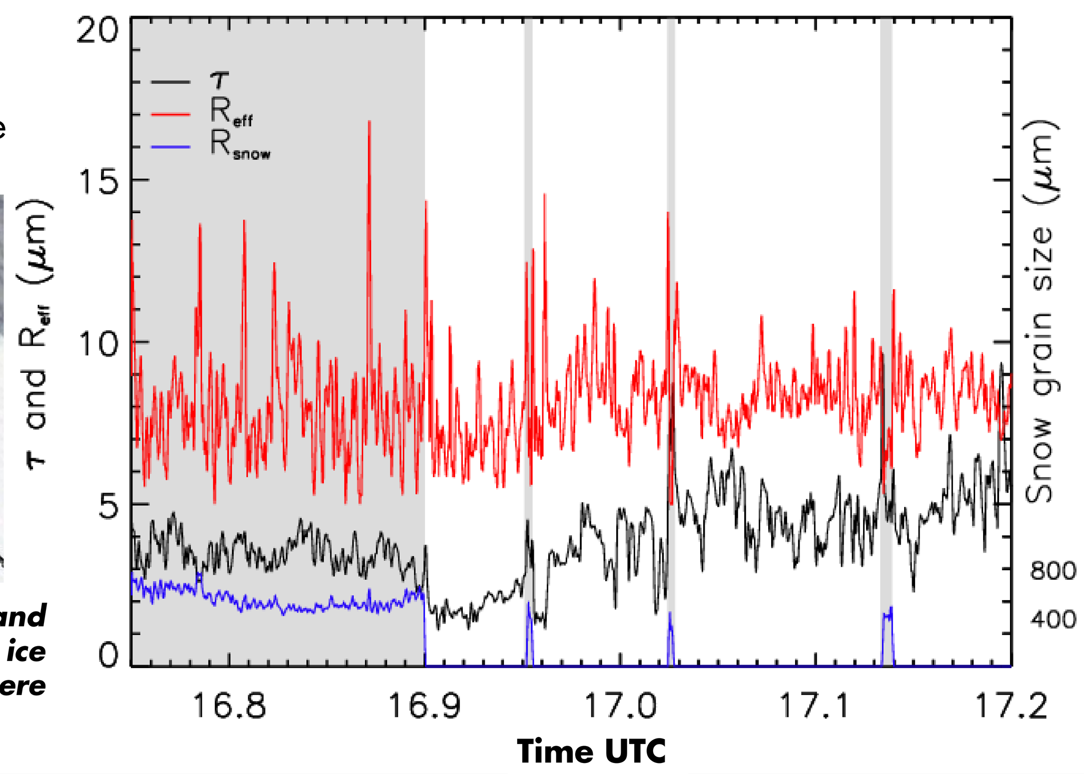

Fig. 10: Time series of retrieved τ, R_{eff}, and R_{snow} along the flight track crossing an ice edge. Grey shaded areas indicate where snow or ice surfaces were located.

6. Outlook

- Uncertainty analysis → Improve wavelength selection
- Validation by in situ observations
- Comparison with satellite observations:
  – Snow retrieval in cloud free areas/days
  – Cloud retrieval over ice free areas
- Application to more cases (RACEPAC 2014)

[1] Brückner, M., B. Pospichal, A. Macke, and M. Wendisch (2014), A new multispectral cloud retrieval method for ship-based solar transmissivity measurements, J. Geophys. Res. Atmos., 119, 11,338–11,354, doi:10.1002/2014JD021775.
[2] Werner F., H. Siebert, P. Pilewskie, T. Schmeissner, R. A. Shaw, and M. Wendisch (2013), New airborne retrieval approach for trade wind cumulus properties under overlying cirrus, J. Geophys. Res. Atmos., 118, 3634–3649, doi:10.1002/jgrd.50334.

Gedruckt im Universitätsrechenzentrum Leipzig